Role of ERK1/2 signaling in congenital valve malformations in Noonan syndrome

Maike Krenz, James Gulick, Hanna E. Osinska, Melissa C. Colbert, Jeffery D. Molkentin, and Jeffrey Robbins[1]

Department of Pediatrics, Division of Molecular Cardiovascular Biology, Cincinnati Children's Hospital Medical Center, Cincinnati, OH 45229-3039

Edited by Eric N. Olson, University of Texas Southwestern Medical Center, Dallas, TX, and approved October 14, 2008 (received for review July 7, 2008)

Noonan syndrome (NS) is the most common nonchromosomal genetic disorder associated with cardiovascular malformations. The most prominent cardiac defects in NS are pulmonary valve stenosis and hypertrophic cardiomyopathy. Gain-of-function mutations in the protein tyrosine phosphatase Shp2 have been identified in 50% of NS families. We created a NS mouse model with selective overexpression of mutant Shp2 (Q79R-Shp2) in the developing endocardial cushions. In our model, Cre recombinase driven by the Tie2 promoter irreversibly activates transgenic Q79R-Shp2 expression in the endothelial-derived cell lineage. Q79R-Shp2 expression resulted in embryonic lethality by embryonic day 14.5. Importantly, mutant embryos showed significantly enlarged endocardial cushions in the atrioventricular canal and in the outflow tract. In contrast, overexpression of wild-type Shp2 protein at comparable levels did not enhance endocardial cushion growth or alter the morphology of the mature adult valves. Expression of Q79R-Shp2 was accompanied by increased ERK1/2 activation in a subset of cells within the cushion mesenchyme, suggesting that hyperactivation of this signaling pathway may play a pathogenic role. To test this hypothesis in vivo, Q79R-Shp2-expressing mice were crossed with mice carrying either a homozygous ERK1 or a heterozygous ERK2 deletion. Deletion of ERK1 completely rescued the endocardial cushion phenotype, whereas ERK2 protein reduction did not affect endocardial cushion size. Constitutive hyperactivation of ERK1/2 signaling alone with a transgenic approach resulted in a phenocopy of the valvular phenotype. The data demonstrate both necessity and sufficiency of increased ERK activation downstream of Shp2 in mediating abnormal valve development in a NS mouse model.

cardiac | heart

Congenital heart defects remain the most common birth defect, occurring in ≈1% of live births (1). In the largest subgroup (25–30%), defects in valvuloseptal development are the underlying cause (2). Genetic analyses of families with congenital heart disease helped define the molecular mechanisms underlying certain valve malformations. In particular, gain-of-function mutations in the protein tyrosine phosphatase Shp2 have recently been discovered in families with Noonan syndrome (NS) (3). In the majority of cases, NS follows autosomal dominant inheritance and is characterized by short stature, facial dysmorphia, skeletal anomalies, and congenital heart disease (4–6). Among the heart defects, pulmonary valve stenosis and hypertrophic cardiomyopathy are most prominent (6, 7). Understanding the exact cellular mechanism(s) by which dysfunction of Shp2 causes valve malformations may provide the basis for future development of novel therapeutic approaches.

Shp2 consists of 2 tandemly arranged src homology 2 (SH2) domains in its N-terminal region, a classic protein tyrosine phosphatase (PTP) domain, and a C-terminal tail (8). The N-SH2 domain is thought to act as a molecular switch regulating Shp2 activity (9). In the inactive conformation, the N-SH2 domain blocks access to the catalytic cleft of the PTP domain (10). Upon binding of phosphotyrosyl ligands, interactions between the N-SH2 and the PTP domains are disrupted, resulting in unfolding and activation of Shp2. Interestingly, many of the NS mutations are located either in the N-SH2 domain or in the facing PTP domain, suggesting that these mutations might permanently disrupt interactions between the 2 domains and thereby force the protein into the active conformation. Energetics-based structural analyses confirmed that for at least some NS mutants, including Q79R, the active conformation of Shp2 is indeed favored, resulting in a gain of Shp2 phosphatase activity (3). In an in vitro assay, we have recently shown a 4.5-fold higher phosphatase activity of Q79R-Shp2 compared with the wild-type protein (11).

Shp2 is ubiquitously expressed and involved in a large number of biological processes and signaling events. Shp2 modulates multiple signaling pathways including the extracellular-regulated kinase (ERK), c-Jun N-terminal kinase (JNK), janus-activated kinase/signal transducer and activator of transcription (JAK/STAT), and nuclear factor-κB (NF-κB) cascades (12, 13). To delineate which pathway might play a role for the pathogenesis of NS-related valve defects, we used a reductionist in vitro approach. In explanted and cultured chick valve primordia, Q79R-Shp2 caused increased cell proliferation via positive modulation of ERK signaling (11). However, correct valve development requires the complex interplay of multiple signals from different tissues together with hemodynamic stimuli (14), and the in vitro assays may be of limited utility to understanding the in vivo situation.

To complicate matters further, we currently have no explanation for the striking cell type dependence of the effects of various NS mutations that has been observed. For example, in a gene-targeted mouse model of NS, only select organ systems and tissues are affected despite ubiquitous expression of Shp2 protein containing a human NS mutation (15). These data represent a particular challenge when studying valve development abnormalities associated with NS because signals from the myocardium, the extracellular matrix, and the endothelium all act in a coordinated fashion to enable correct valve formation (14). With regard to NS patients, it is unclear which cell population actually promotes the pathogenesis of valve defects during embryonic development.

At least 4 different cell populations need to be considered for potential roles in the pathogenesis of valve disease (14): cardiomyocytes, neural crest-derived cells that substantially contribute to the leaflets of the outflow tract valves, endothelial cells that cover all valve primordia, and endothelial-derived cells that make up the majority of mesenchymal cells in all 4 developing valves. We have already obtained in vivo data in mice concerning 3 of these 4 cell populations. In a previous study using cardiomyocyte-specific transgenesis, expression of a NS gain-of-function

Author contributions: M.K. and J.R. designed research; M.K. and H.E.O. performed research; J.G., M.C.C., and J.D.M. contributed new reagents/analytic tools; M.K., H.E.O., and J.R. analyzed data; and M.K. wrote the paper.

The authors declare no conflict of interest.

This article is a PNAS Direct Submission.

[1]To whom correspondence should be addressed. E-mail: jeff.robbins@cchmc.org.

This article contains supporting information online at www.pnas.org/cgi/content/full/0806556105/DCSupplemental.

www.pnas.org/cgi/doi/10.1073/pnas.0806556105

mutation in Shp2, Q79R, before birth had no discernible effect on valve development (16). We have also studied the effects of Q79R-Shp2 expression in the neural crest-derived cells of the outflow tract by using Wnt1-Cre to activate transgenic Q79R-Shp2 expression, but the outflow tract valves developed normally. Furthermore, we have used the Tie2 promoter to drive Q79R-Shp2 expression directly in the endothelium, and we did not see any alterations in valve development (T. Nakamura and J.R., unpublished observations). With this approach, the mesenchymal cells within the endocardial cushions do not express Q79R-Shp2 because the Tie2 promoter is shut off as the endothelial cells at the surface of the cushion undergo endothelial to mesenchymal transformation and migrate into the cushions (17).

Having thus excluded 3 major cell populations as causative for NS-related valve disease, we now focus on the 4th population, the endothelial-derived cells. The first aim of the present work was to generate a mouse model in which Q79R-Shp2 is expressed on the surface of the cushions and in the majority of the cells within the endocardial cushions. A Tie2-Cre-directed approach has already been used for a number of loss-of-function studies focusing on this cell population in the developing valves (18, 19). We used this tool to induce a gain of function by driving Cre recombinase with the Tie2 promoter. This irreversibly activated transgenic Q79R-Shp2 expression in the endothelial-derived cell lineage and resulted in abnormal valve development.

The second aim of our work was then to use this tissue-specific model of NS to investigate signaling events downstream of Q79R-Shp2 in vivo. Based on our earlier findings in cardiomyocytes (16) and explanted endocardial cushions from avian embryos (11), we hypothesized that Q79R-Shp2 would cause inappropriate modulation of the ERK signaling cascade, thereby dysregulating early endocardial cushion formation and growth. We tested both the sufficiency and necessity of intact ERK1/2 activation in early valve development by constitutively activating ERK in the developing cushions and by crossing the Q79R-Shp2 expressors into ERK 1 and ERK2 deletion backgrounds.

Results

Generation of a Tissue-Specific NS Mouse Model. The aim of our work was to generate a tissue-specific model of NS in which the mutated protein is expressed in the majority of mesenchymal cells within the developing valves. Therefore, we used a Cre/loxP recombination system (20) to induce prenatal expression of wild-type or mutant Shp2 (WT-Shp2; Q79R-Shp2) in the endothelial-derived cell lineage. WT or Q79R-Shp2 cDNA was inserted after a CAGCAT cassette [chicken actin promoter (CAG) followed by chloramphenicol acetyltransferase (CAT) cDNA flanked by 2 loxP sites] and used to generate transgenic mice. Under normal conditions, the WT-Shp2 or Q79R-Shp2 is not transcribed because transcription is terminated after the CAT cDNA. However, upon Cre expression in the tissue or cell type of choice, the recombinase excises the CAT cassette including the poly(A) stop sequences and activates transcription of WT-Shp2 or Q79R-Shp2.

To achieve mutant Shp2 expression in the endothelial-derived cell lineage, we mated CAGCAT-Q79R-Shp2 and CAGCAT-WT-Shp2 mice with transgenic mice expressing Cre under the control of the endothelial-specific Tie2 promoter (17). In the double-transgenic (DTG) offspring, this resulted in stable expression of transgenic protein in endothelial cells and endothelial-derived cells, including the mesenchymal cell population of the valve primordia both in the atrioventricular canal (AVC) and in the outflow tract (OFT; Fig. 1 *A–F*). As a control experiment, we also crossed Tie2-Cre mice with mice carrying a CAGCAT-enhanced green fluorescence protein (CAGCAT-eGFP) construct [supporting information (SI) Fig. S1]. In the resulting DTGs, we found pronounced eGFP expression in the entire vascular endothelium, the endocardium, and within the developing endocardial cushions. The distribution of eGFP and the overexpression patterns in the WT-Shp2 and Q79R-Shp2 DTGs was in agreement with previous cell lineage studies both in terms of spatial distribution and prevalence (20–22). In particular, the leaflets of the tricuspid and mitral valves almost entirely consist of cell originating from endothelial cells (21, 22). In contrast, although the leaflets of the aortic and pulmonary valves also contain a large amount of endocardially derived mesenchyme, neural crest-derived cells make a major contribution to these leaflets (22). We used the Tie2-Cre × CAGCAT-eGFP DTGs to quantify the number of cells in the cushion mesenchyme targeted by our approach. Greater than 90% of the mesenchymal cells in the AVC cushions expressed eGFP at embryonic day (E) 13.5 (Fig. 1*H*). In contrast, only 43% of the mesenchymal cells in the proximal OFT cushions were targeted.

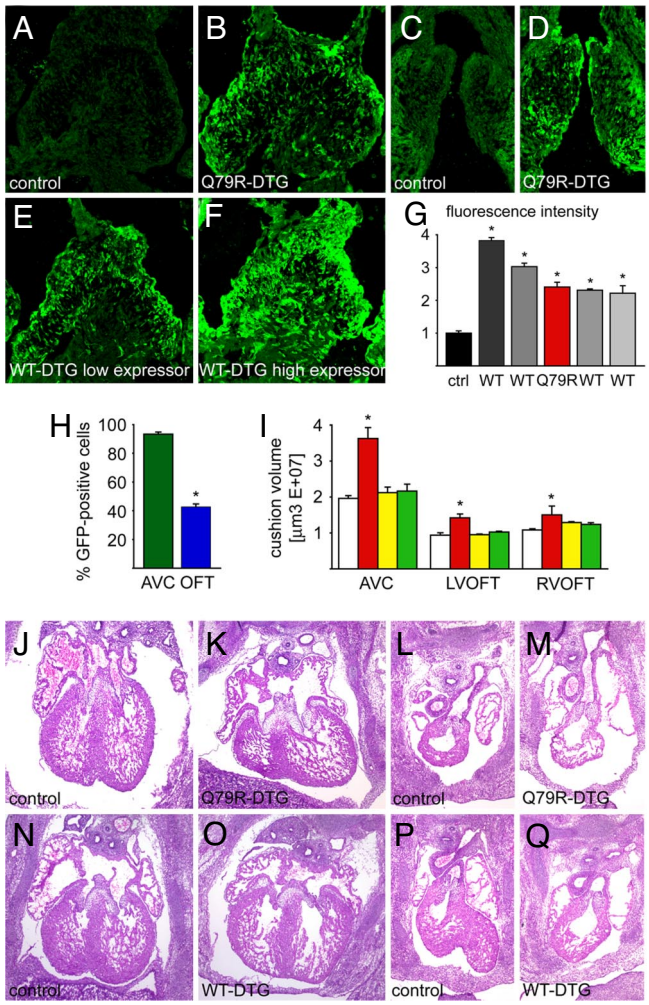

Fig. 1. Endothelial lineage-specific expression of Q79R-Shp2 in the embryonic mouse heart. (*A–F*) Immunostaining for total Shp2 in the septal leaflets of the atrioventricular valves (*A*, *B*, *E*, and *F*) and in the pulmonary valve leaflets (*C* and *D*). (*G*) Quantification and comparison of Shp2 staining in 1 Q79R-Shp2 line (red) and 4 independent WT-Shp2 lines (gray) vs. endogenous levels (control, black) ($n = 2–3$ hearts with 2–4 sections each per group); *, $P < 0.05$ vs. nontransgenic control. (*H*) Percentage of cells positive for GFP in the endocardial cushion mesenchyme of the AVC (green) and OFT (blue); *, $P < 0.05$ vs. AVC group. (*I*) Endocardial cushion volumes in control (white), Q79R-DTG (red), control (yellow), and WT-DTG (green) hearts at E13.5 ($n = 3$ per group; *, $P < 0.05$ vs. control). (*J–Q*) Representative histological sections through AVC and right ventricular OFT leaflets in control, Q79R-, and WT-DTG hearts.

Table 1. Genotype frequencies and cardiac malformations of E13.5 embryos

Genotype	Frequency	Noncompaction	DORV	VSD
Q79R-DTG	7/37 (19%)	4/10	1/10	2/10
Control	30/37 (81%)	0/7	0/7	0/7
WT-DTG (high expressor)	11/43 (26%)	0/3	0/3	0/3
Control	32/43 (74%)	0/3	0/3	0/3
Q79R-DTG;ERK1$^{-/-}$	11/40 (27%)	1/5	1/5	3/5
Control;ERK1$^{-/-}$	29/40 (73%)	0/5	0/5	1/5
Q79R-DTG;ERK2$^{+/-}$	11/117 (9%)	3/4	0/3	4/4
Control;ERK2$^{+/-}$	55/117 (47%)	0/3	0/3	0/3

DORV, double-outlet right ventricle; VSD, ventricular septal defect.

Originally, we generated 3 independent CAGCAT-Q79R-Shp2 lines. The 3 lines showed only small differences in protein overexpression levels and similar phenotypes when crossed to Tie-Cre mice, and we arbitrarily chose 1 line for the experiments shown below.

To quantify total Shp2 protein levels at E13.5, we measured immunofluorescent signal intensities from multiple sections through the AVC cushions by using MetaMorph software (Fig. 1*G*). Q79R-Shp2 protein levels were ≈2.5-fold elevated relative to endogenous Shp2 levels. We were also able to generate multiple WT-Shp2-overexpressing lines, 2 of which expressed WT-Shp2 at approximately the same level as in the Q79R-Shp2 mice, and 2 other lines that expressed WT-Shp2 at slightly higher levels (Fig. 1*G*).

Q79R-Shp2 Expression Results in Aberrant Cushion Formation. To control for the possibility that alterations in the overall stoichiometries of either the Shp2 transcript or protein pools might lead to a phenotype, we first analyzed DTG offspring from Tie2-Cre × CAGCAT-WT-Shp2 crosses. In all lines, WT-DTGs had a normal life span and histologically did not show any cardiac malformations. Even when the highest-expressing WT-Shp2 line was used, no cardiac abnormalities could be detected (Fig. 1 *N–Q*). In contrast, all Q79R-DTG embryos died by E14.5. The frequency of E13.5 Q79R-DTGs was slightly below the expected Mendelian ratio (Table 1), indicating that some of the Q79R-DTGs had already been reabsorbed at this time. All Q79R-DTG embryos at E13.5 were smaller than the control littermates and showed nuchal and back edema, small livers, and hemorrhage. The s.c. edema in the Q79R-DTGs could already be seen at E12.5 and suggests that heart failure could be contributing to embryonic lethality, although, in histological sections, Q79R-DTGs also demonstrated substantial liver necrosis (Fig. S2). We could not detect morphological abnormalities in the embryonic vasculature (Fig. S2) or in the placental vessels (data not shown).

The most striking cardiac phenotype was a significant increase in endocardial cushion size (Fig. 1 *J–M*). By using serial sections, we quantified total volumes of AVC and proximal OFT cushions at E13.5 (Fig. 1*I*). In WT-DTGs, cushion size was normal, whereas in Q79R-DTGs cushion volumes were increased by up to 85%. Consistent with the smaller proportion of mesenchymal cells targeted, OFT cushion volumes increased by only ≈39%. Cardiac malformations such as double-outlet right ventricle, ventricular septal defects, and ventricular noncompaction, were also found with incomplete penetrance (Table 1 and Fig. S3). In the control group, there were no significant differences among nontransgenic, Tie2-Cre, CAGCAT-Q79R-Shp2, or CAGCAT-WT-Shp2 single-transgenic embryos (data not shown).

Both endothelial and mesenchymal cell ultrastructure in DTG AVC cushions appeared normal (Fig. 2 *A–D*). However, we observed higher rates of cell division in DTG embryo sections and quantified BrdU-labeled cells in the endothelial, mesenchymal, and cardiomyocyte cell populations (Fig. 2*I*). Importantly, proliferation was significantly increased in the AVC cushion endothelium and mesenchyme of the Q79R-DTGs but not in the cardiomyocytes. At the same time, the number of TUNEL-positive nuclei in the developing AVC cushions was significantly reduced (see Fig. 4*M*).

To stage the process of valve formation in the Q79R-DTGs, we used immunohistochemistry for differentiation markers. Nuclear NFATc1 was increased in the endothelium overlying the Q79R-DTG endocardial cushions at E13.5 (Fig. 2 *E* and *F*). We also observed that the level of cartilage link protein present in the valve primordia of the Q79R-DTGs was much lower than in the control embryos (Fig. 2 *G* and *H*), indicating that differen-

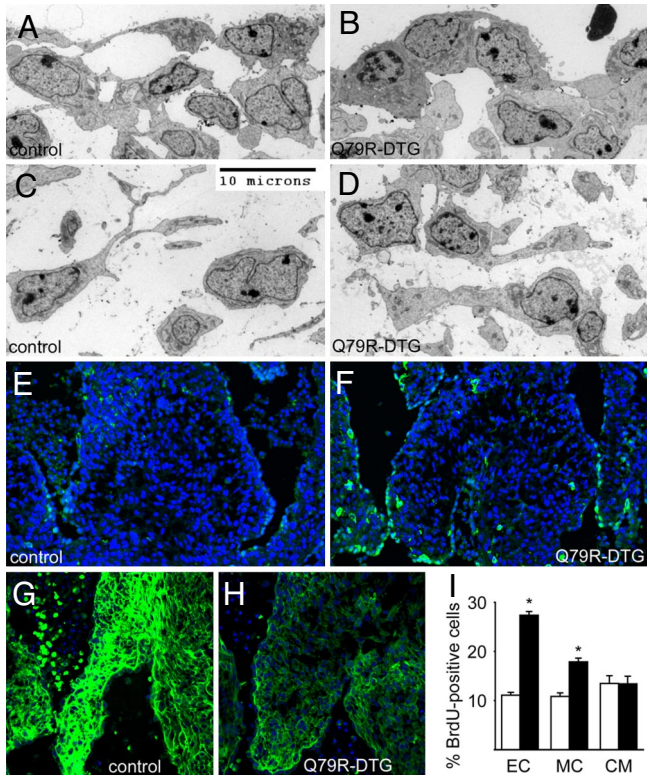

Fig. 2. Ultrastructure, differentiation markers, and mitotic indices in endocardial cushion cells from control and Q79R-DTG embryos at E13.5. (*A* and *B*) Endocardial surface of atrioventricular cushion. (*C* and *D*) Mesenchymal cells within AVC cushions. (*E* and *F*) Immunostaining for NFATc1 (green) together with TO-PRO nuclear stain (blue). (*G* and *H*) Immunostaining for cartilage link protein in septal leaflet of AVC cushions. (*I*) Percentage of BrdU-positive nuclei in the endothelial cell (EC), mesenchymal cell (MC), and cardiomyocyte (CM) population at E13.5 (control, white; Q79R-DTG, black; $n = 3$ hearts per group; *, $P < 0.05$ vs. control).

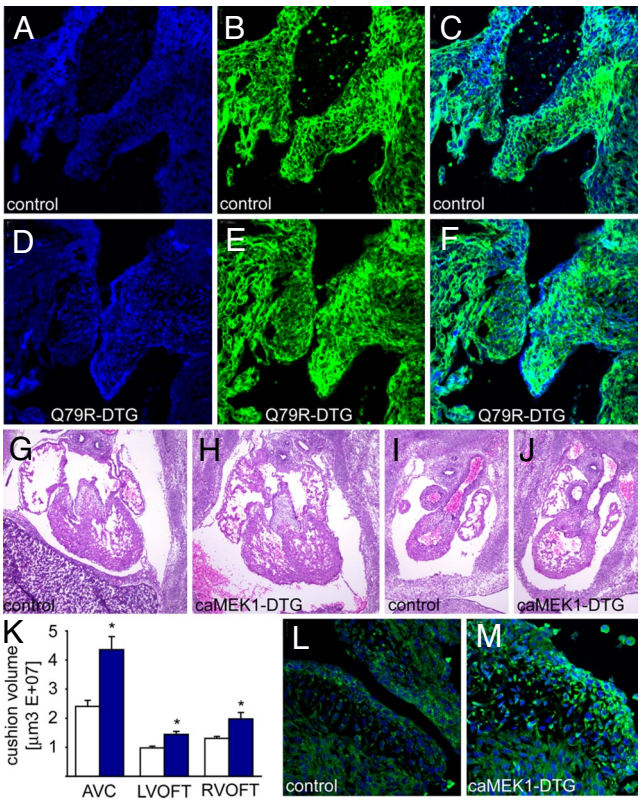

Fig. 3. ERK hyperactivation in endocardial cushions. (*A–F*) Immunostaining for Shp2 (blue) and phospho-ERK1/2 (green) in control and Q79R-DTG E13.5 AVC cushions. (*G–J*) Representative histological sections through AVC and right ventricular OFT leaflets in control and caMEK1-DTG hearts. (*K*) Endocardial cushion volumes in control (white) and caMEK1-DTG (blue) hearts at E13.5 ($n = 3–4$ per group; *, $P < 0.05$ vs. control). (*L* and *M*) Immunostaining for MEK1/2 (green) with TO-PRO nuclear stain (blue) of septal atrioventricular leaflet at E13.5 in control and caMEK1-DTG.

tiation and extracellular matrix remodeling processes had not yet begun.

Constitutive ERK1/2 Activation Is Sufficient to Mimic the NS-Like Phenotype. Previously, we and others (15, 16) showed that the Q79R mutation led to increased ERK1/2 activation in cardiac cell populations. Thus, we determined whether Q79R-Shp2 expression was associated with increased ERK activation in the endocardial cushions (Fig. 3 *B* and *E*). In a subset of AVC cushion cells, expression of Q79R-Shp2 was colocalized with increased ERK1/2 phosphorylation, suggesting that this might indeed be an important part of the underlying pathogenic mechanism. To understand and define the cause-and-effect relationships among Q79R-Shp2 expression, ERK1/2 signaling, and aberrant cushion formation, we subsequently used genetically engineered mice to determine whether isolated, constitutive MEK1 activation within the developing cushions is sufficient to enhance endocardial cushion growth in vivo. By using the same approach as described above, we generated transgenic mice carrying the CAGCAT cassette followed by the cDNA of a constitutively active form of MEK1 (caMEK1). Multiple CAGCAT-caMEK1 transgenic lines were created, and the highest-expressing line was crossed to Tie-Cre mice. No caMEK1-DTGs were observed after birth. At E13.5, caMEK1-DTG embryos were present at the expected Mendelian ratio (data not shown). Serial sections through the embryonic hearts showed substantially enlarged endocardial cushions (Fig. 3 *G–J*). Morphometry confirmed that endocardial cushion volumes were significantly increased (Fig. 3*K*), and the phenotype of the caMEK1-DTGs closely mimicked that of the Q79R-DTGs. Immunohistochemistry for MEK1/2 protein levels in the developing cushions at E13.5 (Fig. 3 *L* and *M*). In the caMEK1-DTGs, total protein levels were ≈1.6-fold elevated compared with the endogenous level (MetaMorph data not shown).

Signaling Through ERK1 Is Necessary to Induce the NS-Like Phenotype. We then tested whether a reduction of ERK1 or ERK2 signaling in the Q79R-Shp2 DTGs could rescue the Q79R-Shp2 phenotype because this could have important therapeutic implications. To this end, we crossed the NS mice into either a homozygous ERK1 deletion background ($ERK1^{-/-}$), a heterozygous ERK1 deletion background ($ERK1^{+/-}$), or into a heterozygous ERK2 deletion background ($ERK2^{+/-}$) (23, 24). Mice carrying a homozygous deletion of ERK1 live into adulthood and are fertile, whereas mice with a homozygous deletion of ERK2 die prenatally (24), necessitating the use of heterozygotes only. In the homozygous ERK1 deletion background, very early embryonic lethality was abolished, restoring the frequency of Q79R-DTGs at E13.5 to the expected Mendelian ratio (Table 1). Representative histological sections in Fig. 4 *A–D* together with the morphometric data in Fig. 4*I* show that the complete loss of ERK1 protein reversed the endocardial cushion phenotype. Partial loss of ERK1 protein resulted in an intermediate reduction of endocardial cushion size (Fig. 4*I*), indicating that this rescue effect is dose-dependent. However, in both the heterozygous and in the homozygous ERK1 deletion backgrounds, the embryos died by E14.5, displaying liver necrosis and nuchal edema (liver necrosis is shown in Fig. S2).

In contrast, a reduction in ERK2 signaling did not affect endocardial cushion volumes (Fig. 4 *F–H* and *J*) and the frequency of double-outlet right ventricle with ventricular septal defect was increased (Table 1). Again, embryos died by E14.5, displaying liver necrosis and nuchal edema. These data indicate that ablation ERK1, but not a reduction in ERK2, can rescue the Q79R-Shp2-induced valve phenotype.

To assess the effects of ERK1/2 deletion on cell proliferation, we quantified BrdU-labeled cells in the endothelial, mesenchymal, and cardiomyocyte cell populations in both crosses (Fig. 4 *K* and *L*). In the homozygous ERK1 deletion background, proliferation rates were normalized, whereas in the heterozygous ERK2 deletion background proliferation in the endothelial and mesenchymal cushion cells was still increased. At the same time, the antiapoptotic effect of Q79R-Shp2 was abolished when ERK1 was deleted, but a reduction in ERK2 protein did not affect the number of TUNEL-positive cells (Fig. 4*M*).

Discussion

The present work demonstrates that overexpression of Q79R-Shp2 in the endothelial-derived cell lineage results in enlarged endocardial cushions caused by increased cell proliferation and reduced apoptosis within the cushion mesenchyme and endothelium. Constitutive hyperactivation of ERK1/2 signaling alone mimicked the valvular phenotype, demonstrating that ERK1/2 activation is sufficient to produce the NS-like phenotype. Furthermore, intact ERK signaling is also necessary for the pathogenesis of the cushion enlargement because deletion of ERK1 completely rescued the endocardial cushion phenotype. ERK2 protein reduction did not affect endocardial cushion size, indicating that either isoform-specific or dose-related effects might be responsible.

The current work substantially adds to our understanding of the pathogenesis of NS, especially with regard to tissue specificity and critical downstream signaling pathways by dissecting cell lineage-specific effects. Considering that we found no effect on valve development when mutant Shp2 was expressed in cardiomyocytes, neural crest-derived cells, or the mesenchymal

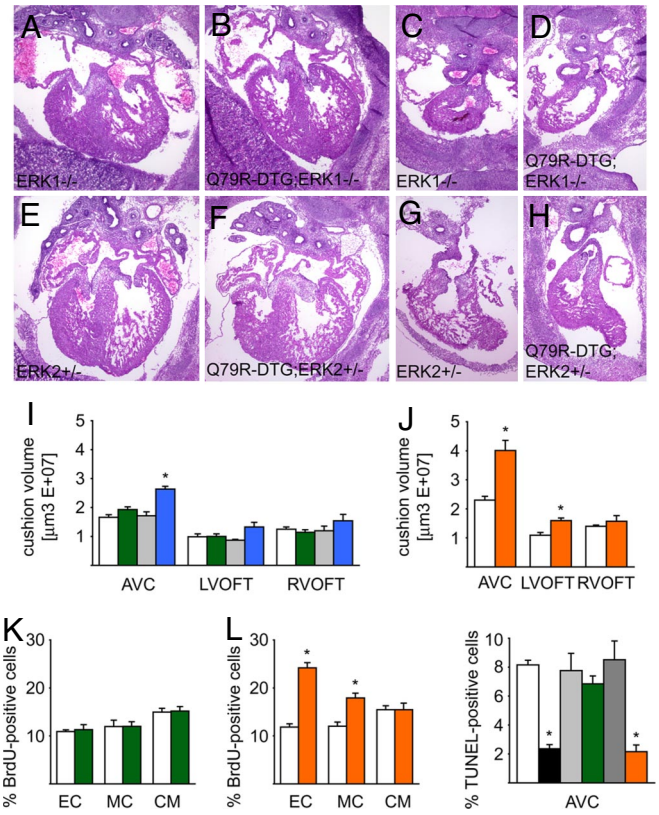

Fig. 4. Deletion of ERK1 but not reduction of ERK2 protein rescues the valve phenotype in Q79R-DTGs. (*A–H*) Representative histological sections through AVC and right ventricular OFT leaflets in ERK1$^{-/-}$, Q79R-DTG;ERK1$^{-/-}$, ERK2$^{+/-}$, and Q79R-DTG;ERK2$^{+/-}$ hearts. (*I*) Endocardial cushion volumes in ERK1$^{-/-}$ (white), Q79R-DTG;ERK1$^{-/-}$ (green), ERK1$^{-/+}$ (gray), and Q79R-DTG;ERK1$^{-/+}$ (blue) hearts at E13.5 (n = 3–5 per group; *, $P < 0.05$ vs. respective control). (*J*) Endocardial cushion volumes in ERK2$^{+/-}$ (white) and Q79R-DTG;ERK2$^{+/-}$ (orange) hearts at E13.5 (n = 3 per group; *, $P < 0.05$ vs. ERK2$^{+/-}$ control). (*K* and *L*) Percentage of BrdU-positive nuclei in the endothelial cell (EC), mesenchymal cell (MC), and cardiomyocyte (CM) population at E13.5 (ERK1$^{-/-}$ and ERK2$^{+/-}$ controls, white; Q79R-DTG;ERK1$^{-/-}$, green; Q79R-DTG;ERK2$^{+/-}$, orange; n = 3–4 hearts per group; *, $P < 0.05$ vs. respective control). (*M*) Percentage of TUNEL-positive nuclei in AVC cushions at E13.5 (control, white; Q79R-DTG, black; ERK1$^{-/-}$, light gray; Q79R-DTG;ERK1$^{-/-}$, green; ERK2$^{+/-}$, dark gray; Q79R-DTG;ERK2$^{+/-}$, orange; n = 3–5 hearts per group; *, $P < 0.05$ vs. respective control).

cells that are endothelial-derived, we conclude that the endothelial-derived cell lineage is the cell population responsible for inducing the NS-like valve phenotype. Previously, a tissue-specific mouse model of neurofibromatosis type 1 demonstrated a similar tissue-specific effect caused by increased ras activation in the endothelial-derived cell lineage (18). Interestingly, in that study neural crest-specific ras activation also did not lead to a cardiac defect.

Because total Shp2 transcript and protein levels were above normal due to the use of transgenesis, we conducted careful control experiments with overexpression of WT-Shp2 protein to demonstrate the validity of our approach. Overexpression of WT-Shp2 at levels even higher than in our Q79R-DTG mice did not result in cardiac abnormalities. Furthermore, we obtained multiple lines both for the WT-Shp2 and Q79R-Shp2 constructs and observed similar phenotypes, indicating that positional effects caused by the DNA insertion were unlikely to play a role.

The embryonic lethality of our NS mouse model is consistent with previous data in which a different gain-of-function NS mutation, D61G-Shp2, was introduced into the endogenous locus by using gene targeting (15). Embryonic lethality was dose-dependent in the D61G mouse model, with 100% lethality at midgestation in the homozygous state. Considering that D61G-Shp2 has 7- to 8-fold increased phosphatase activity whereas Q79R-Shp2 has only a 4.5-fold increased activity compared with wild type but was overexpressed 2.5-fold, our result of complete lethality is very consistent with this earlier study. The D61G-Shp2 mouse phenotype shows increased thickness of mitral and pulmonary valve primordia, double-outlet right ventricle together with ventricular septal defects, ventricular noncompaction, and liver necrosis. On the basis of our Tie2 crosses, it is very likely that the commonalities between the 2 mouse models are caused by alterations in the endothelial-derived cell lineage.

Mechanistically, the cardinal feature of the Q79R-Shp2 valve phenotype is a significantly increased rate of proliferation both in the endothelial cell layer and in the mesenchymal cell population. These data are consistent with our previous in vitro study showing enhanced chick cushion explant outgrowth and cell proliferation in the presence of Q79R-Shp2 (11). Interestingly, increased proliferation in the endothelial layer was accompanied by enhanced nuclear Nfatc1 and decreased expression of cartilage link protein in the Q79R-DTG cushions, indicating that essential elements of growth, differentiation, and remodeling processes are dysregulated. Previously, it has been shown that increased ras activity results not only in increased ERK activation but also enhances activation of Nfatc1 in the endocardial cushion endothelium (18). Moreover, Nfatc1 is thought to mediate proliferation of pulmonary valve endothelial cells induced by vascular endothelial growth factor (25). However, whether this could be a direct effect of the Q79R-Shp2 mutation is not clear. Addition of the calcineurin inhibitor cyclosporin A did not reduce the hyperproliferative effect of Q79R-Shp2 in our previous cushion explant assays (11), implying that activation of Nfatc1 might not be part of the central mechanism.

We hypothesized that dysregulation of ERK signaling is a critical part of the pathomechanism of NS and focused on intracellular signaling events downstream of Shp2. During valve development, ERK activation is dynamically regulated and is particularly enriched in the endocardium overlying the distal tips of the AVC and OFT valves at early and late stages of valve maturation (26). NS gain-of-function mutations in Shp2 can enhance and prolong growth factor signaling (10, 27). Shp2 modulates and regulates signaling through numerous pathways, many of which are active in the developing endocardial cushions and in vitro studies implicated the ERK pathway as a central mechanism (11).

First, we studied whether constitutive activation of ERK1/2 signaling was sufficient to induce a NS-like valve phenotype. A number of activating mutations in proteins downstream of Shp2 and part of the ras–raf–MAPK signaling cascade are associated with human diseases closely related to NS. For example, in cardiofaciocutaneous syndrome that has phenotypic similarities to NS, gain-of-function mutations in *KRAS*, *BRAF*, *MEK1*, and *MEK2* have been identified (28). By constitutively activating ERK1/2 signaling in the mouse valve primordia, we were indeed able to recapitulate the valve phenotype observed in the Q79R-Shp2 embryos. These findings are consistent with our previous study demonstrating that hyperactivation of ERK1/2 signaling resulted in increased cushion explant outgrowth (11). This suggests that there is a common downstream pathway for multiple related diseases, potentially allowing us to treat more than 1 group of patients if a novel approach targeted at downstream signaling can be developed.

Even more important for the design of novel therapeutic avenues is the question of whether intact ERK signaling is required for the pathogenesis of NS. Expression of the activating NS mutant N308D-Shp2 in COS-7 cells enhances ERK2 activity

after EGF stimulation (27), indicating that mutant Shp2 might be acting preferentially via the ERK2 isoform. The MEK1 inhibitors used on Q79R-Shp2 expressing explanted endocardial cushions were not isoform-specific (11), and therefore we chose to cross the Q79R-Shp2 mice into ERK1 and ERK2 deletion backgrounds. Interestingly, deletion of ERK1, but not reduction of ERK2 protein, reversed the valve phenotype induced by Q79R-Shp2. Partial loss of ERK1 led to a partial rescue of the endocardial cushion sizes. ERK2 constitutes 70% of the total ERK1/2 protein content of the heart (29). Assuming that ERK1 and ERK2 are functionally redundant, ERK2 heterozygous mice should be approximately equivalent in effect to the complete targeting of ERK1 (30). However, we did not even see a partial effect in the crosses with heterozygous ERK2 deletion mice, suggesting that ERK1 plays a more prominent and dose-dependent role in the pathogenesis of NS-related valve disease than ERK2.

Materials and Methods

Generation of Mice. All procedures were approved by the Institutional Animal Care and Use Committee. The Q79R-Shp2 mutation was introduced into WT-Shp2 cDNA by using PCR-based mutagenesis. The full-length constructs of WT-Shp2, Q79R-Shp2, and caMEK1 were inserted into the CAGCAT cassette by positional cloning, excised from the vector and used to generate transgenic mice (FVB/N background). To activate transgene expression, transgenic animals were mated with Tie2-Cre mice obtained from Jackson Laboratories. Tie2-Cre, ERK1, and ERK2 deletion mice were crossed into the FVB/N background for at least 7 generations before starting the crosses with the CAGCAT-Q79R-Shp2 mice.

Histology and Morphometry. Embryos were fixed in 4% paraformaldehyde, infused with sucrose, embedded in O.C.T. compound (Tissue-Tek), and cut into 7-μm cryosections. Serial sections through the entire heart were stained with hematoxylin/eosin, and the individual endocardial cushion areas were traced on every 4th section to calculate total cushion volumes. Unpaired *t* tests were used to compare measurements in DTGs vs. controls; $P < 0.05$ was considered significant.

Immunohistochemistry. For immunhistochemistry, frozen sections were stained with anti-Shp2, anti-NFATc1 (Santa Cruz Biotechnologies), anti-phospho-p44/42, anti-MEK1/2 (Cell Signaling), and anti-cartilage link protein (Developmental Studies Hybridoma Bank). Alexa Fluor 488- and 568-conjugated (Molecular Probes) and Cy5-conjugated (Abcam) secondary antibodies were used. To counterstain, we used Alexa Fluor 568-conjugated phalloidin and the nuclear stain TO-PRO-3 iodide (Molecular Probes). Fluorescence intensities were assessed by using MetaMorph Imaging System (Molecular Devices). As region of interest, only septal endocardial cushions of the AVC were selected. Unpaired *t* tests were used to compare signal intensities in DTGs vs. controls, $P < 0.05$ was considered significant.

Electron Microscopy. Transmission electron microscopy (Hitachi 7600) of mouse valve tissue was performed as described in ref. 31.

ACKNOWLEDGMENTS. We thank Katherine E. Yutzey and Michelle Combs for critical advice. This work was supported by National Institutes of Health Grants P01HL69799, P50HL07701, P01HL059408, and R01HL087862 (to J.R.). M.K. was supported by a National Scientist Development grant from the American Heart Association.

1. Hoffman JI, Kaplan S (2002) The incidence of congenital heart disease. *J Am Coll Cardiol* 39:1890–1900.
2. Loffredo CA (2000) Epidemiology of cardiovascular malformations: Prevalence and risk factors. *Am J Med Genet* 97:319–325.
3. Tartaglia M, *et al.* (2001) Mutations in PTPN11, encoding the protein tyrosine phosphatase SHP-2, cause Noonan syndrome. *Nat Genet* 29:465–468.
4. Noonan JA (1968) Hypertelorism with Turner phenotype: A new syndrome with associated congenital heart disease. *Am J Dis Child* 116:373–380.
5. Burch M, *et al.* (1993) Cardiologic abnormalities in Noonan syndrome: Phenotypic diagnosis and echocardiographic assessment of 118 patients. *J Am Coll Cardiol* 22:1189–1192.
6. Marino B, Digilio MC, Toscano A, Giannotti A, Dallapiccola B (1999) Congenital heart diseases in children with Noonan syndrome: An expanded cardiac spectrum with high prevalence of atrioventricular canal. *J Pediatr* 135:703–706.
7. Van der Hauwaert LG, Fryns JP, Dumoulin M, Logghe N (1978) Cardiovascular malformations in Turner's and Noonan's syndrome. *Br Heart J* 40:500–509.
8. Neel BG, Gu H, Pao L (2003) The ''Shp''ing news: SH2 domain-containing tyrosine phosphatases in cell signaling. *Trends Biochem Sci* 28:284–293.
9. Hof P, Pluskey S, Dhe-Paganon S, Eck MJ, Shoelson SE (1998) Crystal structure of the tyrosine phosphatase SHP-2. *Cell* 92:441–450.
10. O'Reilly AM, Pluskey S, Shoelson SE, Neel BG (2000) Activated mutants of SHP-2 preferentially induce elongation of *Xenopus* animal caps. *Mol Cell Biol* 20:299–311.
11. Krenz M, Yutzey KE, Robbins J (2005) Noonan syndrome mutation Q79R in Shp2 increases proliferation of valve primordia mesenchymal cells via extracellular signal-regulated kinase 1/2 signaling. *Circ Res* 97:813–820.
12. Feng GS (1999) Shp2 tyrosine phosphatase: Signaling one cell or many. *Exp Cell Res* 253:47–54.
13. Stein-Gerlach M, Wallasch C, Ullrich A (1998) SHP-2, SH2-containing protein tyrosine phosphatase-2. *Int J Biochem Cell Biol* 30:559–566.
14. Armstrong EJ, Bischoff J (2004) Heart valve development: Endothelial cell signaling and differentiation. *Circ Res* 95:459–470.
15. Araki T, *et al.* (2004) Mouse model of Noonan syndrome reveals cell type- and gene dosage-dependent effects of Ptpn11 mutation. *Nat Med* 10:849–857.
16. Nakamura T, *et al.* (2007) Mediating ERK1/2 signaling rescues congenital heart defects in a mouse model of Noonan syndrome. *J Clin Invest* 117:2123–2132.
17. Schlaeger TM, *et al.* (1997) Uniform vascular endothelial cell-specific gene expression in both embryonic and adult transgenic mice. *Proc Natl Acad Sci USA* 94:3058–3063.
18. Gitler AD, *et al.* (2003) Nf1 has an essential role in endothelial cells. *Nat Genet* 33:75–79.
19. Lincoln J, Kist R, Scherer G, Yutzey KE (2007) Sox9 is required for precursor cell expansion and extracellular matrix organization during mouse heart valve development. *Dev Biol* 305:120–132.
20. Kisanuki YY, *et al.* (2001) Tie2-Cre transgenic mice: A new model for endothelial cell-lineage analysis in vivo. *Dev Biol* 230:230–234.
21. Lincoln J, Alfieri CM, Yutzey KE (2004) Development of heart valve leaflets and supporting apparatus in chicken and mouse embryos. *Dev Dyn* 230:239–250.
22. de Lange FJ, *et al.* (2004) Lineage and morphogenetic analysis of the cardiac valves. *Circ Res* 95:645–654.
23. Pagès G, *et al.* (1999) Defective thymocyte maturation in p44 MAP kinase (Erk1) knockout mice. *Science* 286:1374–1377.
24. Saba-El-Leil MK, *et al.* (2003) Essential role of the MAP kinase ERK2 in mouse trophoblast development. *EMBO Rep* 4:964–968.
25. Johnson EN, *et al.* (2003) NFATc1 mediates vascular endothelial growth factor-induced proliferation of human pulmonary valve endothelial cells. *J Biol Chem* 278:1686–1692.
26. Liberatore CM, Yutzey KE (2004) MAP kinase activation in avian cardiovascular development. *Dev Dyn* 230:773–780.
27. Tartaglia M, *et al.* (2003) Somatic mutations in PTPN11 in juvenile myelomonocytic leukemia, myelodysplastic syndromes, and acute myeloid leukemia. *Nat Genet* 34:148–150.
28. Roberts A, *et al.* (2006) The cardiofaciocutaneous syndrome. *J Med Genet* 43:833–842.
29. Lips DJ, *et al.* (2004) MEK1–ERK2 signaling pathway protects myocardium from ischemic injury in vivo. *Circulation* 109:1938–1941.
30. Purcell NH, *et al.* (2007) Genetic inhibition of cardiac ERK1/2 promotes stress-induced apoptosis and heart failure but has no effect on hypertrophy in vivo. *Proc Natl Acad Sci USA* 104:14074–14079.
31. Fewell JG, *et al.* (1997) A treadmill exercise regimen for identifying cardiovascular phenotypes in transgenic mice. *Am J Physiol* 273:H1595–H1605.